



Visualizing hydrogen sulfide in living cells and zebrafish using a red-emitting fluorescent probe via selenium-sulfur exchange reaction

Xiaoyu Zhang^{a, c, 1}, Wangbo Qu^{c, 1}, Heng Liu^{a, c, **}, Yingying Ma^c, Linlin Wang^c, Qi Sun^{b, ***}, Fabio Yu^{a, *}

^a Institute of Functional Materials and Molecular Imaging, Key Laboratory of Emergency and Trauma, Ministry of Education, Key Laboratory of Hainan Trauma and Disaster Rescue, College of Clinical Medicine, College of Emergency and Trauma, Hainan Medical University, Haikou, 571199, China

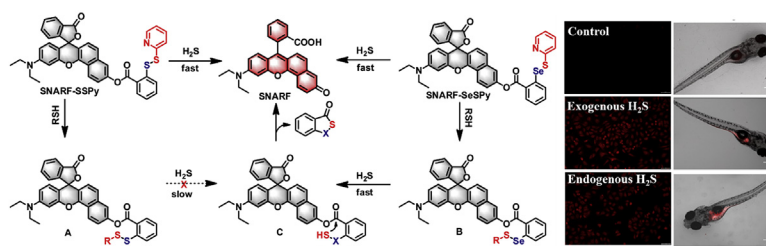
^b Key Laboratory for Green Chemical Process of Ministry of Education and School of Chemistry and Environmental Engineering, Wuhan Institute of Technology, Wuhan, 430205, China

^c Hubei Collaborative Innovation Center for Advanced Organic Chemical Materials, Ministry of Education Key Laboratory for the Synthesis and Application of Organic Functional Molecules & College of Chemistry and Chemical Engineering, Hubei University, Wuhan, 430062, China

HIGHLIGHTS

- Two red-emitting fluorescent probes SNARF-SSPy and SNARF-SeSPy have been designed for efficient detection of H₂S.
- By comparing the two probes, only SNARF-SeSPy exhibited excellent anti-interference even in the presence of high concentration of thiols.
- Results of imaging H₂S in living cells and zebrafish demonstrated that SNARF-SeSPy could be employed to track exogenous and endogenous H₂S in vitro and in vivo.

GRAPHICAL ABSTRACT



ARTICLE INFO

Article history:

Received 11 January 2020

Received in revised form

12 February 2020

Accepted 17 February 2020

Available online 27 February 2020

Keywords:

Hydrogen sulfide
Fluorescent probes
Red emission

ABSTRACT

Hydrogen sulfide (H₂S) is an important endogenous gasotransmitter and has been implicated with a variety of biological processes. The development of an efficient method for monitor H₂S fluctuations in biological systems is of great significance to understand its roles in physiological and pathological conditions. In this work, two red-emitting fluorescent probes SNARF-SSPy and SNARF-SeSPy for H₂S detection with turn-on fluorescence signals were reported. Interestingly, SNARF-SeSPy exhibited excellent anti-interference via dual selenium-sulfur exchange reaction even in the presence of high concentrations of thiols, whereas SNARF-SSPy did not sense H₂S in the same condition. Additionally, in the present of H₂S, SNARF-SeSPy showed a rapid response and excellent sensitivity with a detection limit of

* Corresponding author.

** Corresponding author. Institute of Functional Materials and Molecular Imaging, Key Laboratory of Emergency and Trauma, Ministry of Education, Key Laboratory of Hainan Trauma and Disaster Rescue, College of Clinical Medicine, College of Emergency and Trauma, Hainan Medical University, Haikou, 571199, China.

*** Corresponding author.

E-mail addresses: liuheng11b@hubu.edu.cn (H. Liu), qisun@wit.edu.cn (Q. Sun), fbuyu@yic.ac.cn (F. Yu).

¹ These two authors contributed equally to this work (X. Y. Zhang and W.B. Qu).

<https://doi.org/10.1016/j.aca.2020.02.061>

0003-2670/© 2020 Elsevier B.V. All rights reserved.

1. Introduction

Hydrogen sulfide (H₂S) is widely known as a colorless, toxic gas with rotten egg smell in the past decades. However, H₂S is recently classified as an important gaseous signaling molecule following carbon monoxide (CO) and nitric oxide (NO) [1–4]. Increasing evidences suggest H₂S appears to have protective effects in a diverse array of pathologies, such as anti-inflammation, anti-oxidative stress, regulation of blood pressure and cardiovascular protection [5–8]. Recent studies also confirm endogenous production of H₂S is mainly from enzymes-catalyzed desulfhydration reaction of cysteine and homocysteine in various cell types. These enzymes include cystathionine-β-synthase, cystathionine-γ-lyase, 3-mercapto-sulfurtransferase and cysteine aminotransferase [9–14]. Early literatures report that the whole blood amounts of H₂S is in the range of 35–80 μM [15], as well as the level variations of H₂S are closely correlated with many human diseases such as Alzheimer's disease [16,17] and Down's syndrome [18]. Hence, there is a highly desirable and keen interest in developing efficient methods for real-time tracking the level fluctuation of H₂S and determining its roles in various biological processes.

Several common methods including methylene blue assay [19], gas chromatography-mass spectrometry analysis [20] and sulfide ion-specific electrode [8], have been proposed for H₂S determination in various samples, but these methods can't in situ detect H₂S at the cellular level or in vivo. Fluorescent probes show great potential for solving this issue owing to the high spatiotemporal resolution and good biocompatibility [21–25]. More recently, different strategies including H₂S-mediated nucleophilic addition [26–33], H₂S-mediated thiolysis [34–38], H₂S-mediated reduction of azide and nitro group [39,40] have been exploited to design H₂S probes. Nevertheless, all these strategies are based on the high nucleophilicity and reductibility of H₂S, which will make the developed probes susceptible to interference from other nucleophilic or reduced species under physiological conditions. For example, many H₂S-specific probes containing disulfide linkage have been recently designed, but the main disadvantage of these probes is that they are easily consumed by biothios in vivo, which could cause a decrease in sensitivity of these probes [27–29,31,32]. Consequently, the development of highly selective and sensitive probes for H₂S detection remains challenging.

To solve this problem, we herein designed and synthesized two reaction-based red-emitting probes SNARF-SSPy and SNARF-SeSPy for H₂S specific detection. These two probes displayed off-on fluorescence response to H₂S by utilizing an H₂S-triggered cascade nucleophilic reaction to release the fluorophore SNARF. Interestingly, by comparing SNARF-SSPy and SNARF-SeSPy, we found only the fluorescence of SNARF-SeSPy enhanced significantly in the coexistence of high concentrations of thiols. We reasoned that selenium was easier attacked by H₂S than sulfur due to its high electrophilicity, which made SNARF-SeSPy capable of releasing the fluorophore SNARF via dual selenium-sulfur exchange reaction to achieve fluorescence enhancement. Furthermore, SNARF-SeSPy was successfully applied for monitoring exogenous/endogenous H₂S in living cells and zebrafish, which provided a powerful tool for studying the function of H₂S in living systems.

2. Experimental section

2.1. General information

All the reagents and solvents in this work were purchased from commercial suppliers and used without further purification. Ultrapure water (18.2 MΩ · cm) was used for all spectral analysis. ¹H NMR and ¹³C NMR spectra were recorded by a Varian 600 MHz spectrometer with TMS as an internal standard. MS data (ESI) was obtained on an Agilent 1260–6224 LC/MS. Absorption spectra were acquired in a Shimadzu UV-2700 spectrophotometer. Fluorescence spectra were measured on an Agilent Cary Eclipse spectrophotometer.

2.2. General procedure for spectra measurement

The stock solutions of two probes (2 mM) were prepared in dimethyl sulfoxide. Analyte stock solutions (10 mM) of methionine (Met), glycine (Gly), Arginine (Arg), proline (Pro), cysteine (Cys), homocysteine (Hcy), glutathione (GSH), Na₂S · 9H₂O (H₂S), Na₂S₂O₃ (S₂O₃²⁻), Na₂SO₃ (SO₃²⁻), Na₂SO₄ (SO₄²⁻), NaCl (Cl⁻), NaClO (ClO⁻), MgSO₄ (Mg²⁺), Al(NO₃)₃ (Al³⁺), Ca(NO₃)₂ (Ca²⁺), Fe(NO₃)₃ (Fe³⁺) were prepared in freshly 50 mM PBS buffer. The stock solution of cetrimonium bromide (CTAB, 10 mM) was prepared in ethanol. 30 μl of stock solution of CTAB, 15 μl of stock solution of probe and appropriate volume of analyte stock solution were added into PBS buffer (50 mM, pH 7.4) to give a final volume being 3 ml. The fluorescence excitation wavelength was 580 nm with excitation and emission slits of 5 nm.

2.3. Fluorescence imaging in live cells

A549 cells were cultured in Dulbecco's modified eagle's medium (DMEM) medium supplemented with 10% (v/v) fetal bovine serum and 1% (v/v) penicillin-streptomycin at 37 °C in an atmosphere containing 5% carbon dioxide. The cells were seeded in a 12-well plate for 24 h. The cells were incubated with different concentrations of H₂S (0, 50, 100 μM) in PBS buffer (pH 7.4, containing 50 μM CTAB) for 30 min followed by incubation with SNARF-SeSPy (10 μM) for 30 min. In vivo cell imaging experiment, the cells pretreated with 20 μM of sodium nitroprusside dehydrate (SNP) for 30 min were incubated with SNARF-SeSPy (10 μM) for 30 min. The cell images were taken by an inverted fluorescence microscope (Olympus IX71, Japan) after the cells were washed three times with PBS buffer.

2.4. Fluorescence imaging in zebrafish

The zebrafish post-fertilization was purchased from Eze-Rinka Company (Nanjing, China). Then the zebrafish were cultured in 10 ml of embryonic medium supplemented with 1-phenyl-2-thiourea in a beaker at 30 °C for 96 h. The zebrafish were incubated with different concentrations of H₂S (0, 100, 200 μM) for 30 min followed by incubation with SNARF-SeSPy (10 μM) for 30 min. Next, the zebrafish pretreated with 100 μM of SNP for 30 min were incubated with SNARF-SeSPy (10 μM) for 30 min. The zebrafish were washed three times with PBS buffer prior to

fluorescence imaging. All fluorescence images were obtained on a stereomicroscope (Olympus SZX16, Japan).

2.5. Synthesis of SNARF-SSPy

A mixture of SNARF (131 mg, 0.3 mmol, 1 equiv.), compound 1 (94 mg, 0.36 mmol, 1.2 equiv.), 1-(3-dimethylaminopropyl)-3-ethylcarbodiimide hydrochloride (115 mg, 0.6 mmol, 2 equiv.) and 4-dimethylaminopyridine (36.6 mg, 0.3 mmol, 1equiv.) in 10 ml methylene chloride was stirred at room temperature under Argon. The reaction was monitored with TLC. After the reaction was completed, methylene chloride was evaporated followed by column chromatography on silica gel using ethyl acetate/hexane = 1/3 to give the desired product as a red solid (105 mg, yield 51%). SNARF-SSPy ^1H NMR (600 MHz, CDCl_3): δ 8.69 (d, $J = 9.0$ Hz, 1H), 8.48 (d, $J = 4.6$ Hz, 1H), 8.36 (d, $J = 7.9$ Hz, 1H), 8.05 (d, $J = 7.6$ Hz, 1H), 8.01 (d, $J = 8.1$ Hz, 1H), 7.72 (s, 1H), 7.67–7.54 (m, 6H), 7.42 (d, $J = 8.8$ Hz, 1H), 7.37 (d, $J = 7.6$ Hz, 1H), 7.18 (d, $J = 7.6$ Hz, 1H), 7.10–7.09 (m, 1H), 6.81 (d, $J = 8.7$ Hz, 1H), 6.68–6.66 (m, 2H), 6.45–6.44 (m, 1H), 3.41 (q, $J = 7.0$ Hz, 4H), 1.22 (t, $J = 7.0$ Hz, 6H); ^{13}C NMR (150 MHz, CDCl_3): δ 169.67, 164.74, 158.87, 153.58, 152.36, 149.78, 149.60, 147.46, 141.54, 137.30, 134.97, 134.89, 133.87, 132.06, 129.53, 128.92, 126.95, 126.25, 126.11, 125.88, 125.21, 124.87, 124.29, 124.05, 122.62, 122.10, 121.34, 121.01, 119.73, 118.73, 112.90, 108.96, 97.72, 44.50, 12.51; LC-MS m/z : $\text{C}_{40}\text{H}_{30}\text{N}_2\text{O}_5\text{S}_2$ $[\text{M}+\text{H}]^+$ calcd for 683.1674 found 683.1827.

2.6. Synthesis of SNARF-SeSPy

A mixture of SNARF (219 mg, 0.5 mmol, 1 equiv.), compound 2 (187 mg, 0.6 mmol, 1.2 equiv.), 1-(3-dimethylaminopropyl)-3-ethylcarbodiimide hydrochloride (191 mg, 1 mmol, 2 equiv.) and 4-dimethylaminopyridine (61 mg, 0.5 mmol, 1equiv.) in 15 ml methylene chloride was stirred at room temperature under Argon. The reaction was monitored with TLC. After the reaction was completed, methylene chloride was evaporated followed by column chromatography on silica gel using ethyl acetate/hexane = 1/3 to give the desired product as a red solid (85 mg, yield 23%). SNARF-SeSPy ^1H NMR (600 MHz, CDCl_3): δ 8.70 (d, $J = 9.1$ Hz, 1H), 8.44–8.43 (m, 1H), 8.39 (d, $J = 7.7$ Hz, 1H), 8.13 (d, $J = 8.2$ Hz, 1H), 8.05 (d, $J = 7.6$ Hz, 1H), 7.70 (s, 1H), 7.65 (t, $J = 7.4$ Hz, 1H), 7.61 (t, $J = 7.4$ Hz, 1H), 7.57–7.50 (m, 4H), 7.43–7.39 (m, 2H), 7.17 (d, $J = 7.6$ Hz, 1H), 7.04–7.02 (m, 1H), 6.81 (d, $J = 8.6$ Hz, 1H), 6.67–6.65 (m, 2H), 6.41 (d, $J = 8.9$ Hz, 1H), 3.40 (q, $J = 7.0$ Hz, 4H), 1.21 (t, $J = 7.1$ Hz, 6H); ^{13}C NMR (150 MHz, CDCl_3): δ 169.67, 166.20, 158.35, 153.60, 152.35, 149.69, 149.57, 149.52, 147.46, 138.87, 137.14, 134.92, 134.89, 134.23, 131.99, 129.51, 128.88, 127.84, 126.93, 126.48, 126.33, 125.31, 124.85, 124.40, 124.02, 122.58, 122.19, 121.73, 121.16, 120.65, 118.68, 113.00, 108.93, 104.91, 97.65, 84.19, 44.45, 12.53; LC-MS m/z : $\text{C}_{40}\text{H}_{30}\text{N}_2\text{O}_5\text{SSe}$ $[\text{M}+\text{H}]^+$ calcd for 731.1119 found 731.1173.

3. Results and discussion

3.1. Probe design

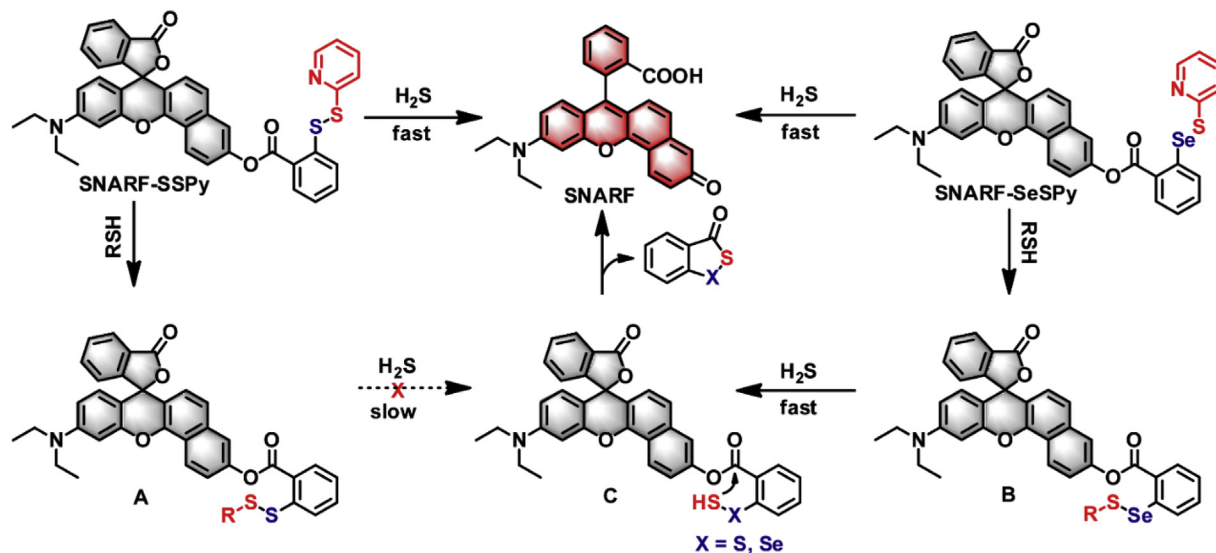
The synthetic strategy of SNARF-SSPy and SNARF-SeSPy was illustrated in Fig. S1. The structures of SNARF-SSPy and SNARF-SeSPy were confirmed by ^1H NMR, ^{13}C NMR and MS (Fig. S2–S7). Compared with short-wavelength fluorophore, seminaphthorhodafluor (SNARF) with long-wavelength (>600 nm) was available for fluorescence imaging because of its merits of the decrease tissue autofluorescence and photodamage [41–45]. In this design, we synthesized two fluorescent probes SNARF-SSPy and SNARF-SeSPy, in which pyridyl disulfide (–SSPy) and pyridyl selenenyl sulfide (–SeSPy) were incorporated on SNARF by an ester

linker, respectively. As depicted in Scheme 1, both SNARF-SSPy and SNARF-SeSPy could undergo tandem nucleophilic reaction to release the red-emitting SNARF fluorophore. Nevertheless, when high concentration thiols were present, SNARF-SSPy containing disulfide (–S–S–) linkage only underwent the first nucleophilic substitution to form intermediate A. SNARF-SeSPy containing selenenyl sulfide (–Se–S–) linkage could first react with thiols to obtain intermediate B, followed by reaction with H_2S to give –Se–SH intermediate C and finally underwent the intramolecular cyclization to release a ring-opening fluorophore SNARF. The major reaction products of SNARF-SeSPy with H_2S were identified as the fluorophore SNARF and cyclic acyl selenylsulfides by ESI-MS analysis (Fig. S8).

3.2. Spectral response of the designed probes

The anti-interference ability is essential for the bioimaging application of the designed fluorescent probes. With the two probes SNARF-SSPy and SNARF-SeSPy in hand, we first compared the selectivity of two probes SNARF-SSPy and SNARF-SeSPy in the presence of potential biorelevant species. As depicted in Fig. 1A, not only common amino acids (Met, Gly, Arg, Pro, Cys, Hcy, GSH) but also anions ($\text{S}_2\text{O}_3^{2-}$, SO_3^{2-} , SO_4^{2-} , Cl^- , ClO^-) and cations (Mg^{2+} , Al^{3+} , Ca^{2+} , Fe^{3+}) showed no to little fluorescence off-on response. When SNARF-SSPy and SNARF-SeSPy were treated with H_2S (using Na_2S as an equivalent), drastic increases in fluorescence were observed, which demonstrated that the two probes could serve as candidates for H_2S detection. However, when we treated the two probes with high concentration of thiols (Cys, Hcy, GSH) and H_2S , SNARF-SSPy showed negligible fluorescence change while SNARF-SeSPy induced a significant fluorescence increase. The results indicated that SNARF-SeSPy could detect H_2S in the biological thiols pool and exhibited better anti-interference than most of the reported H_2S probes (Table S1). We speculated that the reason for this test results was that the reactivity of intermediate B with H_2S was much higher than that of intermediate A. Meanwhile, the color of the two probes solution changes in the presence of thiols and H_2S were also displayed in Fig. 1A. After addition of thiols and H_2S , SNARF-SeSPy compared with SNARF-SSPy was still capable of visual detecting H_2S under room light and 365 UV light. These findings demonstrated the –Se–S– linkage introduced in the designed H_2S probe enabled to effectively avoid the consumption by thiols and had the potential for application in bioimaging.

Next, we examined the ability of SNARF-SeSPy to respond H_2S by absorption and emission spectra. As expected, the free probe was weakly absorbance and fluorescence owing to ring-closed spirolactam form of SNARF. After the addition of a range of different concentrations of H_2S to the probe solution, the major absorption peaks emerged at 572 nm gradually increased and a pronounced fluorescence enhancement at 635 nm was obtained, which were attributed to ring-opening form of SNARF (Fig. 1B and 1C). An excellent linear relationship resided between fluorescence intensities at 635 nm and H_2S concentrations ranging from 0 μM to 20 μM . According to the equation ($F_{635\text{ nm}} = 39.28 \times [\text{Na}_2\text{S}] \mu\text{M} - 48.06$, $r = 0.9957$), the detection limit ($\text{LOD} = 3\sigma/k$) of SNARF to H_2S was estimated to be 34 nM, which suggested SNARF-SeSPy was capable of sensitively detecting H_2S in vitro. Subsequently, the reaction kinetics of SNARF-SeSPy for H_2S was investigated. As can be seen from Fig. 1D, the fluorescence intensity at 635 nm of free probe remained approximately constant. In contrast, the addition of H_2S triggered a significant fluorescence enhancement, as well as the fluorescence intensity achieved an approximate maximum value within 20 min, implying that SNARF-SeSPy was a fast fluorescent light-up probe for H_2S and suitable for bioimaging. Similarly, the reaction between SNARF-SSPy and H_2S was also completed within



Scheme 1. Sensing mechanism of SNARF-SSPy and SNARF-SeSPy toward H_2S .

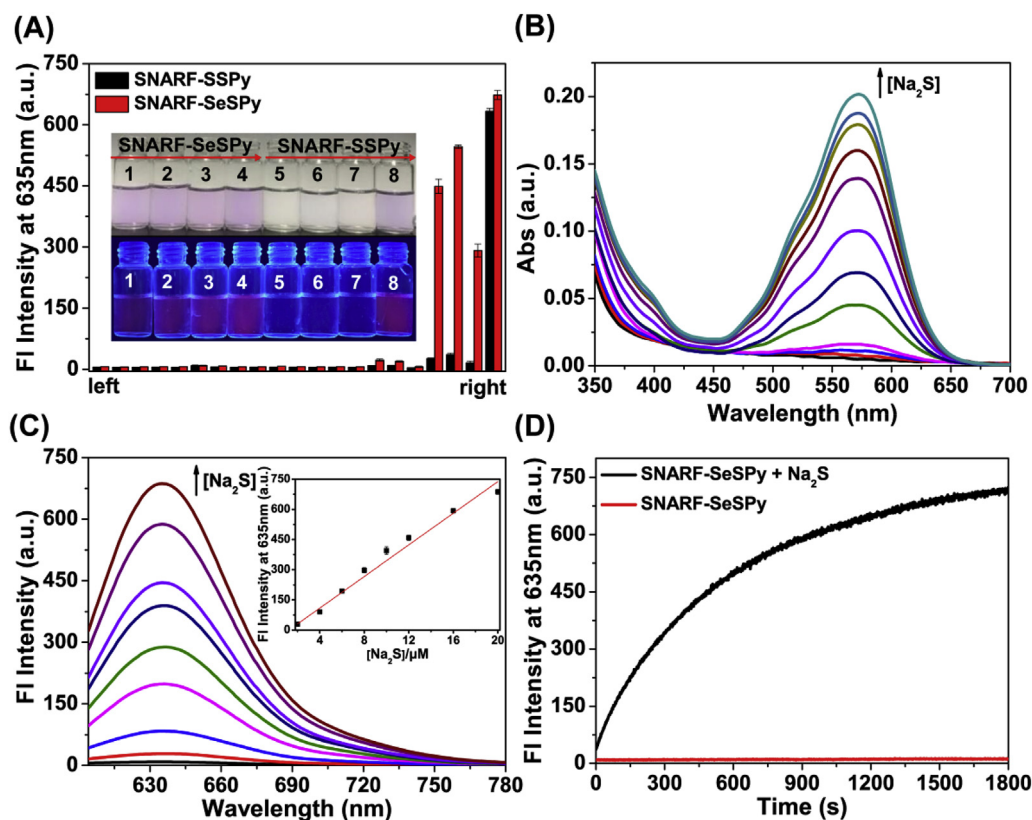


Fig. 1. (A) The selectivity of SNARF-SSPy and SNARF-SeSPy (10 μM) toward potential bio-relevant species. From left to right: probe alone; Met (200 μM), Gly (200 μM), Arg (200 μM), Pro (200 μM), $\text{S}_2\text{O}_3^{2-}$ (100 μM), SO_3^{2-} (100 μM), SO_4^{2-} (100 μM), Cl^- (100 μM), ClO^- (100 μM), Mg^{2+} (100 μM), Al^{3+} (100 μM), Ca^{2+} (100 μM), Fe^{3+} (100 μM), Cys (1 mM), Hcy (200 μM), GSH (1 mM), Cys (1 mM) + Na_2S (50 μM), Hcy (200 μM) + Na_2S (50 μM), GSH (1 mM) + Na_2S (50 μM), Na_2S (50 μM). Inset: photograph of the two probes SNARF-SeSPy (1–4)/SNARF-SSPy (5–8) in the presence of 1 mM Cys + 50 μM Na_2S (1, 5), 200 μM Hcy + 50 μM Na_2S (2, 6), 1 mM GSH + 50 μM Na_2S (3, 7), 50 μM Na_2S (4, 8) under room light (top row) or 365 nm UV light (second row). (B) UV-vis absorption spectra of SNARF-SeSPy (10 μM) upon gradual addition of Na_2S from 0 to 50 μM . (C) Fluorescence titration graph of SNARF-SeSPy upon treatment with Na_2S from 0 to 20 μM . Each spectrum was recorded 20 min post Na_2S addition. Inset: plot of the fluorescence intensities at 635 nm of SNARF-SeSPy versus Na_2S concentrations. (D) Time-dependent fluorescence measures of SNARF-SeSPy after the addition of 50 μM of Na_2S .

5 min (Fig. S9). We also evaluated the sensing properties of the probe for H_2S at different pH values (Fig. S10). The fluorescence of SNARF-SeSPy was very weak and stable over a pH range of 3–10. When H_2S was added to the probe solution, the fluorescence was

significantly enhanced in the pH range of 6–10. These results revealed that SNARF-SeSPy could be applied for H_2S detection in physiological condition.

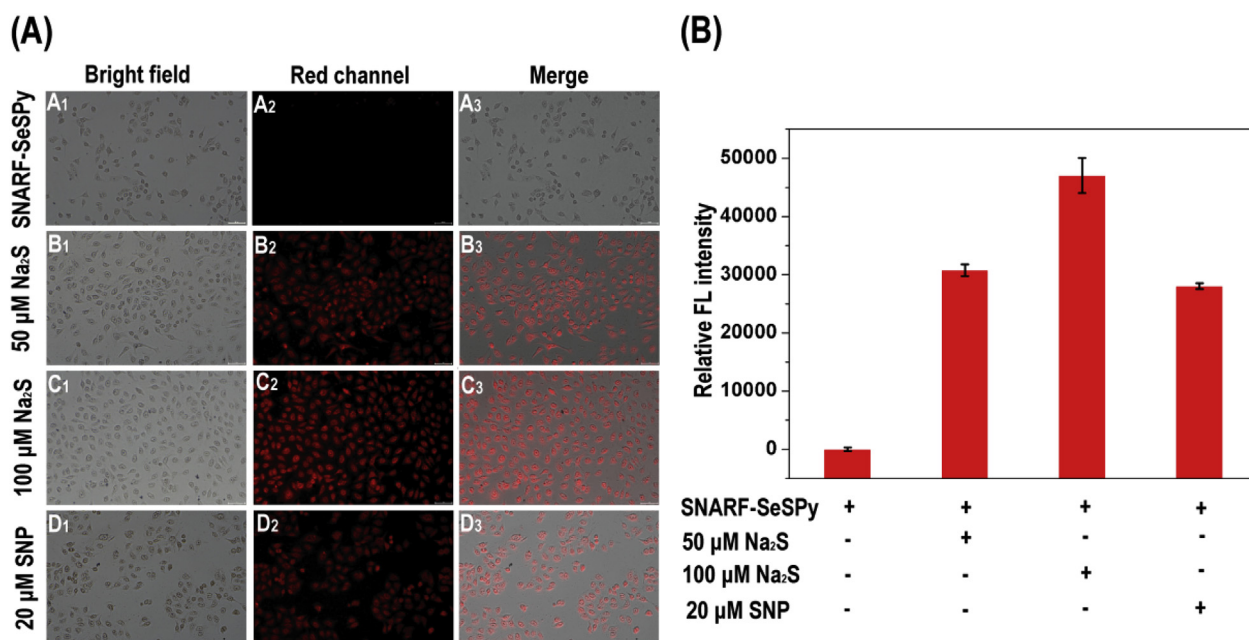


Fig. 2. (A) Fluorescence images of A549 cells. (A₁–A₃) The cells were stained with SNARF-SeSPy (10 μ M) for 30 min; (B₁–B₃) the cells pretreated with Na₂S (50 μ M) for 30 min were treated with SNARF-SeSPy (10 μ M) for 30 min; (C₁–C₃) the cells pretreated with Na₂S (100 μ M) for 30 min were treated with SNARF-SeSPy (10 μ M) for 30 min; (D₁–D₃) the cells pretreated with SNP (20 μ M) for 30 min were treated with SNARF-SeSPy (10 μ M) for 30 min (A₁, B₁, C₁, D₁) brightfield image; (A₂, B₂, C₂, D₂) red channel; (A₃, B₃, C₃, D₃) merged images. Scale bar = 50 μ m. (B) Relative fluorescence intensity of the corresponding fluorescence images (A₂, B₂, C₂, D₂). Values represent mean standard error (n = 3). (For interpretation of the references to color in this figure legend, the reader is referred to the Web version of this article.)

3.3. Imaging of living cells

CCK-8 assay was performed to investigate the cytotoxicity of SNARF-SeSPy on living A549 cells. As illustrated in Fig. S11, after treatment with various concentrations of the probe for 12 h, the cell viability only changed slightly, suggesting the probe featured low

cytotoxicity. On the basis of the outstanding performance of SNARF-SeSPy for H₂S detection, we then evaluated the application of this probe in living cells. As a control, the A549 cells stained with SNARF-SeSPy (10 μ M) for 30 min exhibited weak fluorescence; however, the presence of H₂S (50 μ M) resulted in a large increase in red fluorescence intensity. When the cells were preincubated with

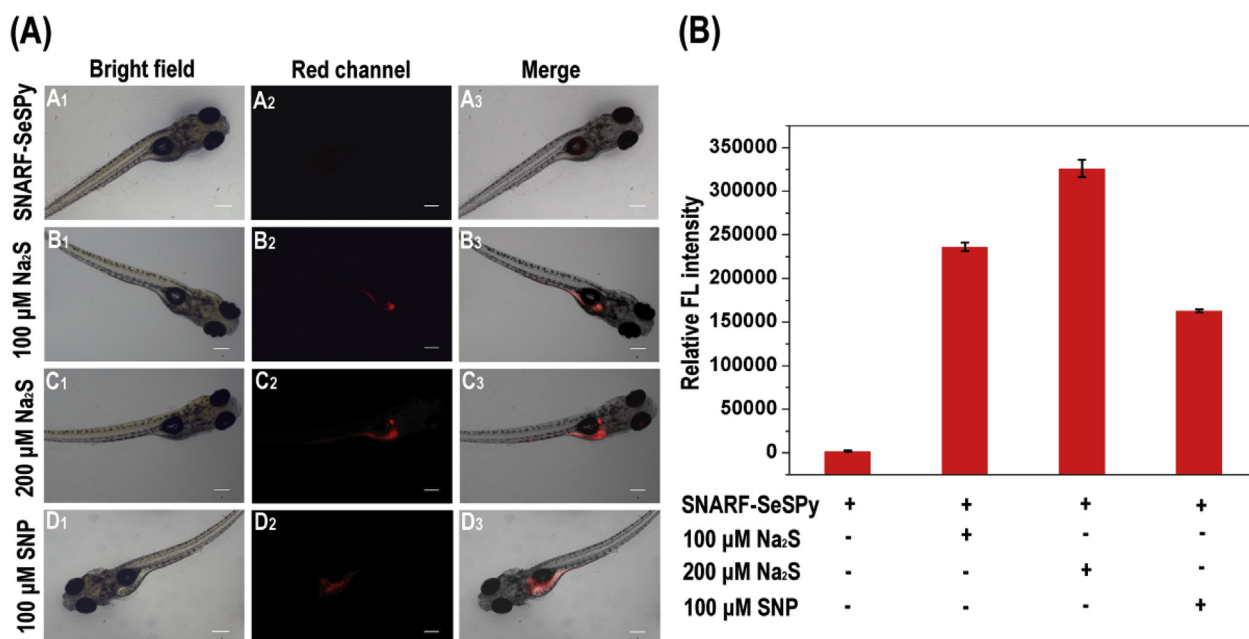


Fig. 3. (A) Fluorescence images of zebrafish. (A₁–A₃) The zebrafish was incubated with SNARF-SeSPy (10 μ M) for 30 min; (B₁–B₃) the zebrafish pretreated with Na₂S (100 μ M) for 30 min was treated with SNARF-SeSPy (10 μ M) for 30 min; (C₁–C₃) the zebrafish pretreated with Na₂S (200 μ M) for 30 min was treated with SNARF-SeSPy (10 μ M) for 30 min; (D₁–D₃) the cells pretreated with SNP (100 μ M) for 30 min was treated with SNARF-SeSPy (10 μ M) for 30 min (A₁, B₁, C₁, D₁) brightfield image; (A₂, B₂, C₂, D₂) red channel; (A₃, B₃, C₃, D₃) merged images. Scale bar = 200 μ m. (B) Relative fluorescence intensity of the corresponding fluorescence images (A₂, B₂, C₂, D₂). Values represent mean standard error (n = 3). (For interpretation of the references to color in this figure legend, the reader is referred to the Web version of this article.)

H₂S (100 μM) and then incubated with the probe (10 μM), the fluorescence intensity further increased. To verify whether the probe was capable to image endogenous H₂S in living cells, we sequentially incubated the cells with 20 μM of SNP (a NO donor capable of inducing endogenous H₂S production by upregulate the enzyme activity of cystathionine-β-synthase and cystathionine-γ-lyase) and 10 μM of SNARF-SeSPy. A remarkable increase in fluorescence was noticed compared to the control group (Fig. 2). These results illustrated that SNARF-SeSPy was suited to monitor exogenous and endogenous H₂S fluctuations in living cells.

3.4. Imaging of living zebrafish larvae

To enlarge the range of application, we set out to explore the ability of SNARF-SeSPy to image H₂S in vivo. We chose the zebrafish larvae as a model organism because the genes of zebrafish and human had 70% homology (Fig. 3). The zebrafish showed almost undetected red fluorescence after treatment with SNARF-SeSPy. After the zebrafish were incubated with various amounts of H₂S (100 or 200 μM), followed by incubation with SNARF-SeSPy (10 μM), varying degrees of fluorescence increases emerged in red channel, which demonstrated the probe could detect exogenous H₂S. Visualization of endogenous H₂S by exogenous SNP stimulation was also performed. In the presence of SNP, the zebrafish presented an obvious red fluorescence from pelvic fin to pectoral fin, which was due to the reaction of SNARF-SeSPy with endogenous H₂S in vivo. These data demonstrated that SNARF-SeSPy potentially served as a probe for the detection of exogenous and endogenous H₂S in vivo.

4. Conclusion

In summary, we reported two red-emitting fluorescent probes capable of detecting H₂S. Our results demonstrated that –Se-S- linkage could effectively improve the anti-interference of the designed probe to detect H₂S compared with –S-S- linkage. The probe SNARF-SeSPy could react with H₂S via dual selenium-sulfur exchange reaction to release the fluorophore, thus showing fluorescence turn-on response. Moreover, the probe was able to respond H₂S with high selectivity, sensitivity and anti-interference. Results of imaging H₂S in living cells and zebrafish demonstrated that SNARF-SeSPy enabled to track exogenous and endogenous H₂S in vitro and in vivo. We expected that –Se-S- linkage could be used as a valuable response site to construct H₂S probes for the diagnosis of H₂S-related diseases in the future.

Declaration of competing interest

The authors declare that they have no known competing financial interests or personal relationships that could have appeared to influence the work reported in this paper.

CRedit authorship contribution statement

Xiaoyu Zhang: Methodology, Data curation, Writing - original draft. **Wangbo Qu:** Methodology, Data curation, Writing - original draft. **Heng Liu:** Conceptualization, Supervision, Project administration, Funding acquisition. **Yingying Ma:** Validation, Writing - review & editing. **Linlin Wang:** Validation, Writing - review & editing. **Qi Sun:** Supervision, Project administration, Funding acquisition. **Fabiao Yu:** Supervision, Project administration, Funding acquisition.

Acknowledgement

This work was supported by the National Natural Science Foundation of China (NSFC. 21961010, 21602051, 21775162, 21804102), Talent Program of Hainan Medical University (Grants XRC190034, XRC180006), and Hundred-Talent Program (Hainan 2018).

Appendix A. Supplementary data

Supplementary data to this article can be found online at <https://doi.org/10.1016/j.aca.2020.02.061>.

References

- [1] J.M. Fukuto, S.J. Carrington, D.J. Tantillo, J.G. Harrison, L.J. Ignarro, B.A. Freeman, et al., Small molecule signaling agents: the integrated chemistry and biochemistry of nitrogen oxides, oxides of carbon, dioxygen, hydrogen sulfide, and their derived species, *Chem. Res. Toxicol.* 25 (2012) 769–793.
- [2] C. Szabo, Roles of hydrogen sulfide in the pathogenesis of diabetes mellitus and its complications, *Antioxid. Redox. Signal.* 17 (2011) 68–80.
- [3] K.R. Olson, A practical look at the chemistry and biology of hydrogen sulfide, *Antioxid. Redox. Signal.* 17 (2011) 32–44.
- [4] L. Li, P. Rose, P.K. Moore, Hydrogen sulfide and cell signaling, *Annu. Rev. Pharmacol.* 51 (2011) 169–187.
- [5] H.X. Zhang, S.J. Liu, X.L. Tang, G.L. Duan, X. Ni, X.Y. Zhu, et al., H₂S attenuates LPS-induced acute lung injury by reducing oxidative/nitrative stress and inflammation, *Cell. Physiol. Biochem.* 40 (2016) 1603–1612.
- [6] A.L. King, D.J. Lefer, Cytoprotective actions of hydrogen sulfide in ischaemia–reperfusion injury, *Exp. Physiol.* 96 (2011) 840–846.
- [7] S. Sowmya, Y. Swathi, A.L. Yeo, M.L. Shoon, P.K. Moore, M. Bhatia, Hydrogen sulfide: regulatory role on blood pressure in hyperhomocysteinemia, *Vasc. Pharmacol.* 53 (2010) 138–143.
- [8] R.T. Wedding, Sulfide Determination: Ion-specific Electrode, *Method. Enzymol.* Academic Press, 1987, pp. 29–31.
- [9] H. Liu, M.N. Radford, C.-t. Yang, W. Chen, M. Xian, Inorganic hydrogen polysulfides: chemistry, chemical biology and detection, *Br. J. Pharmacol.* 176 (2019) 616–627.
- [10] O. Kabil, R. Banerjee, Enzymology of H₂S biogenesis, decay and signaling, *Antioxid. Redox. Signal.* 20 (2013) 770–782.
- [11] S. Bruce King, Potential biological chemistry of hydrogen sulfide (H₂S) with the nitrogen oxides, *Free. Radical. Biol. Med.* 55 (2013) 1–7.
- [12] B.D. Paul, S.H. Snyder, H₂S signalling through protein sulphydration and beyond, *Nat. Rev. Mol. Cell. Biol.* 13 (2012) 499–507.
- [13] O. Kabil, R. Banerjee, Redox biochemistry of hydrogen sulfide, *J. Biol. Chem.* 285 (2010) 21903–21907.
- [14] L.F. Hu, M. Lu, P.T. Hon Wong, J.S. Bian, Hydrogen sulfide: neurophysiology and neuropathology, *Antioxid. Redox. Signal.* 15 (2010) 405–419.
- [15] R.r. Hyšpler, A. Tichá, M. Indrová, Z. Zadák, L. Hyšplerová, J. Gasparič, et al., A simple, optimized method for the determination of sulphide in whole blood by GC–MS as a marker of bowel fermentation processes, *J. Chromatogr. B* 770 (2002) 255–259.
- [16] B.D. Paul, S.H. Snyder, Gasotransmitter hydrogen sulfide signaling in neuronal health and disease, *Biochem. Pharmacol.* 149 (2018) 101–109.
- [17] H.J. Wei, X. Li, X.Q. Tang, Therapeutic benefits of H₂S in Alzheimer's disease, *J. Clin. Neurosci.* 21 (2014) 1665–1669.
- [18] P. Kamoun, M.C. Belardinelli, A. Chabli, K. Lallouchi, B. Chadefaux-Vekemans, Endogenous hydrogen sulfide overproduction in down syndrome, *Am. J. Med. Genet. A* 116A (2003) 310–311.
- [19] R.R. Moest, Hydrogen sulfide determination by the methylene blue method, *Anal. Chem.* 47 (1975) 1204–1205.
- [20] V. Varlet, N. Giuliani, C. Palmiere, G. Maujean, M. Augsburger, Hydrogen sulfide measurement by headspace-gas chromatography-mass spectrometry (HS-GC-MS): application to gaseous samples and gas dissolved in muscle, *J. Anal. Toxicol.* 39 (2014) 52–57.
- [21] J. Ning, W. Wang, G. Ge, P. Chu, F. Long, Y. Yang, et al., Target enzyme-activated two-photon fluorescent probes: a case study of cyp3a4 using a two-dimensional design strategy, *Angew. Chem. Int. Ed.* 58 (2019) 9959–9963.
- [22] W. Chen, T. Matsunaga, D.L. Neill, C.T. Yang, T. Akaike, M. Xian, Rational design of a dual-reactivity-based fluorescent probe for visualizing intracellular HSNO, *Angew. Chem. Int. Ed.* 58 (2019) 16067–16070.
- [23] M. Gao, F. Yu, C. Lv, J. Choo, L. Chen, Fluorescent chemical probes for accurate tumor diagnosis and targeting therapy, *Chem. Soc. Rev.* 46 (2017) 2237–2271.
- [24] W. Chen, A. Pacheco, Y. Takano, J.J. Day, K. Hanaoka, M. Xian, A single fluorescent probe to visualize hydrogen sulfide and hydrogen polysulfides with different fluorescence signals, *Angew. Chem. Int. Ed.* 55 (2016) 9993–9996.
- [25] Y. Wu, Q. Wang, T. Wu, W. Liu, H. Nan, S. Xu, et al., Detection and imaging of hydrogen sulfide in lysosomes of living cells with activatable fluorescent quantum dots, *ACS Appl. Mater. Interfaces* 10 (2018) 43472–43481.

- [26] Y. Wang, C.T. Yang, S. Xu, W. Chen, M. Xian, Hydrogen sulfide mediated tandem reaction of selenenyl sulfides and its application in fluorescent probe development, *Org. Lett.* 21 (2019) 7573–7576.
- [27] J. Wang, Y. Wen, F. Huo, C. Yin, Based 'successive' nucleophilic substitution mitochondrial-targeted H₂S red light emissive fluorescent probe and its imaging in mice, *Sensor. Actuator. B Chem.* 297 (2019) 126–773.
- [28] H. Wang, D. Yang, R. Tan, Z.J. Zhou, R. Xu, J.F. Zhang, et al., A cyanine-based colorimetric and fluorescence probe for detection of hydrogen sulfide in vivo, *Sensor. Actuator. B Chem.* 247 (2017) 883–888.
- [29] J. Kang, F. Huo, C. Yin, A novel ratiometric fluorescent H₂S probe based on tandem nucleophilic substitution/cyclization reaction and its bioimaging, *Dyes. Pigments.* 146 (2017) 287–292.
- [30] W. Chen, S. Xu, J.J. Day, D. Wang, M. Xian, A general strategy for development of near-infrared fluorescent probes for bioimaging, *Angew. Chem. Int. Ed.* 56 (2017) 16611–16615.
- [31] B. Peng, W. Chen, C. Liu, E.W. Rosser, A. Pacheco, Y. Zhao, et al., Fluorescent probes based on nucleophilic substitution–cyclization for hydrogen sulfide detection and bioimaging, *Chem. Eur. J.* 20 (2014) 1010–1016.
- [32] C. Liu, J. Pan, S. Li, Y. Zhao, L.Y. Wu, C.E. Berkman, et al., Capture and visualization of hydrogen sulfide by a fluorescent probe, *Angew. Chem. Int. Ed.* 50 (2011) 10327–10329.
- [33] Q. Zhao, J. Kang, Y. Wen, F. Huo, Y. Zhang, C. Yin, "Turn-on" fluorescent probe for detection of H₂S and its applications in bioimaging, *Spectrochim. Acta Mol. Biomol. Spectrosc.* 189 (2018) 8–12.
- [34] S. Gong, E. Zhou, J. Hong, G. Feng, Nitrobenzoxadiazole ether-based near-infrared fluorescent probe with unexpected high selectivity for H₂S imaging in living cells and mice, *Anal. Chem.* 91 (2019) 13136–13142.
- [35] M. Qian, L. Zhang, Z. Pu, J. Xia, L. Chen, Y. Xia, et al., A NIR fluorescent probe for the detection and visualization of hydrogen sulfide using the aldehyde group assisted thiolysis of dinitrophenyl ether strategy, *J. Mater. Chem. B.* 6 (2018) 7916–7925.
- [36] B. Gu, W. Su, L. Huang, C. Wu, X. Duan, Y. Li, et al., Real-time tracking and selective visualization of exogenous and endogenous hydrogen sulfide by a near-infrared fluorescent probe, *Sensor. Actuator. B Chem.* 255 (2018) 2347–2355.
- [37] S. Ding, W. Feng, G. Feng, Rapid and highly selective detection of H₂S by nitrobenzofurazan (NBD) ether-based fluorescent probes with an aldehyde group, *Sensor. Actuator. B Chem.* 238 (2017) 619–625.
- [38] H. Niu, B. Ni, K. Chen, X. Yang, W. Cao, Y. Ye, et al., A long-wavelength-emitting fluorescent probe for simultaneous discrimination of H₂S/Cys/GSH and its bio-imaging applications, *Talanta* 196 (2019) 145–152.
- [39] V.S. Lin, W. Chen, M. Xian, C.J. Chang, Chemical probes for molecular imaging and detection of hydrogen sulfide and reactive sulfur species in biological systems, *Chem. Soc. Rev.* 44 (2015) 4596–4618.
- [40] F. Yu, X. Han, L. Chen, Fluorescent probes for hydrogen sulfide detection and bioimaging, *Chem. Commun.* 50 (2014) 12234–12249.
- [41] W. Qu, C. Niu, X. Zhang, W. Chen, F. Yu, H. Liu, et al., Construction of a novel far-red fluorescence light-up probe for visualizing intracellular peroxynitrite, *Talanta* 197 (2019) 431–435.
- [42] W. Qu, K. Li, D. Han, X. Zhong, C. Chen, X. Liang, et al., Lysosome-targetable red-emitting ratiometric fluorescent probe for hypobromous acid imaging in living cells, *Sensor. Actuator. B-Chem.* 297 (2019) 126–826.
- [43] J. Ning, T. Liu, P. Dong, W. Wang, G. Ge, B. Wang, et al., Molecular design strategy to construct the near-infrared fluorescent probe for selectively sensing human cytochrome p450 2J2, *J. Am. Chem. Soc.* 141 (2019) 1126–1134.
- [44] Y.V. Suseela, N. Narayanaswamy, S. Pratihari, T. Govindaraju, Far-red fluorescent probes for canonical and non-canonical nucleic acid structures: current progress and future implications, *Chem. Soc. Rev.* 47 (2018) 1098–1131.
- [45] Z. Guo, S. Park, J. Yoon, I. Shin, Recent progress in the development of near-infrared fluorescent probes for bioimaging applications, *Chem. Soc. Rev.* 43 (2014) 16–29.